

# Wing Design for Minimum Drag with Practical Constraints

Tad McGeer\*

Simon Fraser University, Burnaby, British Columbia

General design characteristics of wings that offer minimum drag while satisfying a variety of practical constraints are sought, including primarily a constraint upon structural weight. The essential elements of aerodynamics and structures, when combined with analytical optimization, lead to a series of solutions for lift, chord, and thickness distributions across the span. Although the optimized wings do not differ radically from current practice in these distributions, they can offer significantly lower drag. For high subsonic wings of given structural weight, elasticity, and maximum load factor, forward rather than aft sweep promises a reduction in cruise induced drag of about 10%. Wings whose weight is a large fraction of the total lift, as in sailplanes, may realize larger reductions.

## Nomenclature

$A_m$	= $m$ th harmonic of the spanwise lift distribution, Eq (2)
$A_{Em}$	= $m$ th harmonic of the incremental lift due to aeroelastic bending
$A_{Pm}$	= $m$ th harmonic of the 1 g additional lift distribution
$A_{Pm}^*$	= $m$ th harmonic of the constant speed additional lift distribution, Eq (2)
$b$	= wing span
$\bar{b}$	= span relative to the elliptical reference wing, Eq (13)
$B_m$	= defined in Eq (13)
$B_m'$	= defined in Eq (32)
$B_m''$	= defined in Eq (35)
$c$	= section chord
$C_m$	= $m$ th harmonic of the chord distribution, Eq (5)
$C_l$	= section lift coefficient
$C_{l\perp}$	= $C_l / \cos^2 \Lambda$
$C_{l\text{ lim}}$	= upper bound on section lift coefficient
$C_L$	= wing lift coefficient
$C_{L^E}$	= incremental $C_L$ due to aeroelastic bending at 1 g
$D_i$	= induced drag, Eq (8)
$\bar{D}$	= induced drag relative to the reference wing Eq (9)
$\ell$	= lift/unit span
$L$	= total wing lift
$M$	= bending moment, Eq (11)
$M_m$	= $m$ th harmonic of the bending moment, Eq (12)
$M_{cc}$	= crest critical Mach number, Eq (19)
$q$	= dynamic pressure
$S$	= wing area
$t/c$	= section thickness to chord ratio
$w$	= wing weight/unit span, Eq (10)
$\bar{W}_S$	= area weight/total lift
$y$	= spanwise coordinate
$\alpha$	= angle of attack
$\epsilon_E$	= twist due to elastic deflection, Eq (22)
$\epsilon_{TR}$	= slope of the elastic axis at the tip of the reference wing
$\eta$	= spanwise coordinate Eq (1)
$\Lambda$	= sweep angle
$\nu$	= Lagrange multiplier

$\tau$	= section $t/c$
$\tau_{\text{ref}}$	= $t/c$ of the reference wing
$\chi$	= dimensionless chord Eq (4)
<b>Subscripts</b>	
CD	= condition at which the $M_{cc}$ constraint is imposed
DD	= condition at which the induced drag is minimized
E	= due to elastic twist
MG	= condition at which maximum loading is experienced
lg	= unaccelerated condition
$\perp$	= component normal to the quarter chord line

## Introduction

THIS paper presents algorithms for choosing the spanwise distributions of lift, chord and thickness to chord ratio ( $t/c$ ) of wings. The choices are optimal in that they minimize induced drag while satisfying constraints on structural weight, parasite or compressibility drag and the spanwise  $C_l$  distribution. These constraints play a key role; for example, they cause the optimal lift distribution to depart from the familiar elliptical form. Application of the algorithms is restricted to wings of at least moderate aspect ratio and designed for subsonic cruising flight. Within that restriction, the results are dimensionless and cast in terms of a small set of constraints and parameters so they can be used for designs ranging from sailplanes to high speed transports.

## Prior Work

The literature holds a rich history of analyses in this spirit. Preceding work has focused on optimizing the lift distribution only, with variations on the constraint used to account for structural weight. Jones<sup>1</sup> fixed aerodynamic bending moment at the wing root, while de Young<sup>2</sup> fixed the moment at an arbitrary span position. Prandtl<sup>3</sup> integrated the bending moment across the span instead. Klein and Viswanathan<sup>4</sup> added a constraint on integrated shear. Löbert<sup>5</sup> solved the problem with a constraint on integrated moment/thickness ( $M/t$ ). All of these solutions favor shifting lift inboard relative to an elliptical distribution to permit larger span and so lower drag. Table 1 lists typical drags indicated by these solutions relative to the elliptical standard. Löbert's integrated  $M/t$  most accurately represents the amount of material in a uniformly stressed cantilever beam; notice that it must involve the wing's  $t/c$  and planform. In Ref 6, the same weight constraint was applied to a system of two lifting

Received Feb 13, 1984; revision received May 1, 1984. Copyright © 1984 by Tad McGeer. Published by the American Institute of Aeronautics and Astronautics with permission.

\*Assistant Professor, Faculty of Engineering Science, Member AIAA.

surfaces. In this case the lift on each surface was fixed but the structural material was distributed between them for best effect. Reference 6 also gives a solution for the optimal chord distribution. It is important to note that the actual values of the wing's lift and weight are irrelevant to all of these analyses; what matters is that they are held constant in the optimizations.

### New Solutions

The algorithms discussed herein extend these solutions through the following new features: First, provision is made for minimizing induced drag at a  $C_L$  different from that in the critical loading condition ( $C_{L_{MG}}$ ). It turns out that a design which minimizes drag at the maximum  $g$   $C_L$ —typically near  $C_{L_{max}}$ —often has extraordinarily high drag at cruise  $C_L$ 's because the spanwise lift distribution changes over the flight envelope. Second, aeroelastic bending of swept wings (which causes the lift distribution to vary with load factor) is taken into account approximately. Third, an upper bound on the spanwise  $C_l$  distribution is imposed at  $C_{L_{MG}}$ . This prevents the optimization from selecting vanishing chord near the tip. Fourth,  $t/c$  is optimized subject to a constraint on parasite drag or compressibility drag. This constraint keeps  $t/c$  bounded. Fifth, the bending moment relief due to the wing's own weight is included. (Actually, this last feature is significant only for those rare cases in which the wing's weight exceeds about 15% of the total lift.)

Combinations of the last two features lead to three distinct algorithms: light low speed; light high speed; and heavy low speed. "Light" means bending moment relief is excluded. "Low speed" means that parasite drag is constrained; "high speed" means that compressibility drag is constrained. Each algorithm has component lift, chord, and  $t/c$  solutions. The solutions are analytical; in combination they comprise a set of nonlinear simultaneous equations for the optimal wing geometry. Complete derivation and discussion of the various solutions is given by McGeer<sup>7</sup>; only the essential features and results are presented herein. We begin by outlining the mathematical model upon which the optimizations are based. The light wing design formulas and evaluation procedure follow; those for the heavy wing are more complex and best left to Ref. 7. Then characteristic results of applying all three design procedures are reviewed. A particularly provocative result is the apparent superiority of forward sweep for high speed wings; this raises a concern about flutter which is addressed in the final section.

An incidental note before proceeding: One naturally wonders whether minimizing induced drag while holding parasite or compressibility drag fixed is a reasonable strategy since one really wants to minimize total drag. In fact, a true minimization of total drag calls for making the wing thinner and giving up some span, but the optimal lift, chord, and (scaled)  $t/c$  distributions change only slightly. Reference 7 discusses this point in more detail. The advantage of our formulation is that it is simpler but still quite practical.

### Mathematical Representation of Wings

These introductory claims of minimizing one physical quantity while satisfying constraints on several other physical quantities are rather cavalier. In reality we are dealing with mathematical representations for all of these things. In order to determine the value of the results one must assess the physical fidelity of the representations. This section outlines the wing model in sufficient detail to indicate the physical effects which are included in our analysis and to introduce the terms in which the design algorithms are cast. The model consists of expressions for the optimizing variables—the lift, chord, and  $t/c$  distributions; the optimized quantity—induced drag; and the constraints.

### Optimizing Variables

#### Lift

The lift distribution is expressed as a truncated Fourier series. The spanwise variable is

$$\theta \triangleq \cos^{-1} \eta \triangleq \cos^{-1} [2y/b] \quad (1)$$

The series, with dimensionless coefficients, is

$$\ell(\theta) = \frac{2qSC_L}{b} \sum_{\text{odd}}^M A_m \sin m\theta$$

$$A_m = \frac{b}{\pi qSC_L} \int_0^\pi \ell(\theta) \sin m\theta d\theta \quad (2)$$

Only the first term in the series contributes to the total lift; fixing the lift makes  $A_1 = 2/\pi$ . The rest of the coefficients can be chosen freely. Any given wing naturally chooses those associated with its additional lift distribution, which is generated if the wing has no twist. The additional series coefficients are denoted by  $A_{P_m}$ . If one wants a different lift distribution, one must twist the wing. But the amount of twist required is proportional to  $C_L$ . Since one cannot vary the twist with  $C_L$ , the series coefficients will vary instead. The variation is given by

$$A_m = \frac{C_{L_{DD}}}{C_L} A_{DD_m} + \left(1 - \frac{C_{L_{DD}}}{C_L}\right) A_{P_m} \quad (3)$$

This formula is based upon the quasisteady aerodynamic approximation, which applies throughout. Here  $A_{DD_m}$  denotes the  $m$ th coefficient at some drag design  $C_{L_{DD}}$ . Those familiar with the terminology will recognize that  $A_{DD_m}$  includes both basic and additional lift components.

#### Chord

In dimensionless form,

$$\chi(\theta) = (b/S)c(\theta) \quad (4)$$

In the optimization, one must account for the effect of chord variations on the  $A_{P_m}$ ,  $m=3,5$ . For that it is convenient to use a series from

$$c(\theta) = \frac{4}{\pi} \frac{S}{b} \sum_{\text{odd}}^M C_m \sin m\theta$$

$$C_m = \frac{b}{2S} \int_0^\pi c(\theta) \sin m\theta d\theta \quad (5)$$

Then the additional lift variation with planform is approximately

$$\Delta A_{P_m} = \frac{\partial A_{P_m}}{\partial C_m} \Delta C_m \quad (6)$$

This approximation neglects some smaller terms; however, the optimization is quite insensitive to this entire quantity so they are not missed.

#### Thickness to Chord Ratio

$$\text{Notation: } \tau(\theta) \triangleq \frac{t}{c}(\theta) \quad (7)$$

**Optimized Quantity: Induced Drag**

As long as the total lift is nonzero induced drag is given in general by the well-known series

$$D_i = \frac{\pi}{4} \frac{L^2}{qb^2} \sum_{\text{odd}}^M m A_m^2 \quad (8)$$

Inspection reveals that with span fixed, drag is minimized by making  $A_m = 0$  for  $m = 3, 5$ . This corresponds to an elliptical lift distribution. A central concept in our analysis is that by shifting the lift inboard relative to the elliptical form, a larger span is allowed for the same weight, and the drag may be reduced. The drag relative to the elliptical standard is

$$\bar{D} = \frac{1}{\bar{b}^2} \frac{\pi^2}{4} \sum_{\text{odd}}^M m A_m^2 = \frac{1}{\bar{b}^2} \left( 1 + \frac{\pi^2}{4} \sum_3^M m A_m^2 \right) \quad (9)$$

where  $\bar{b}$  is the relative span

**Constraints****Structural Weight**

Structurally, the wing is treated as a uniformly stressed, simple beam. The bending moment is carried by material distributed according to

$$\frac{dw}{dy} = k \sec \Lambda \frac{M(\theta)}{(t/c)(\theta)c(\theta)} \quad (10)$$

(An independent wing weight component, the area weight, appears in the heavy wing analysis. It is distributed in proportion to local chord.) The aerodynamic bending moment can be calculated by integrating the lift distribution which produces the following series:

$$M(\theta) = \sec \Lambda \frac{bL}{2} \sum_{\text{odd}}^M A_m M_m(\theta) \quad (11)$$

These dimensionless moment components are given explicitly by

$$\begin{aligned} M_1(\theta) &= \frac{1}{8} \left( 3 \sin \theta + \frac{\sin 3\theta}{3} \right) - \frac{\theta \cos \theta}{2} \\ M_m(\theta) &= \frac{1}{4} \left( \frac{\sin(m+2)\theta}{(m+2)(m+1)} - \frac{2}{m^2-1} \sin m\theta \right. \\ &\quad \left. + \frac{\sin(m-2)\theta}{(m-2)(m-1)} \right) \quad m \geq 2 \end{aligned} \quad (12)$$

Another integration, this time of the weight distribution, Eq (10), gives the total bending weight. The integral scales with  $b^3$ . Since it is desired to fix the weight we can use the result to find the allowable span. It is best non-dimensionalized by the span of a reference wing with elliptical lift and chord distributions, and constant  $t/c$ . The relative span then satisfies

$$\frac{1}{\bar{b}^3} = \sum_{\text{odd}}^M A_{MG_m} B_m \quad (13)$$

where

$$B_m = \frac{2\tau_{\text{ref}}}{(8/9) - (\pi/4)} \int_0^{\pi/2} \frac{M_m(\theta)}{\tau \chi(\theta)} \sin \theta d\theta \quad (14)$$

The  $A_{MG_m}$  are the coefficients in the series for lift at  $C_{L_{MG}}$

 **$C_l$  Bound**

$C_l(\theta)/C_L$  follows from the lift series Eq (2):

$$\frac{C_l}{C_{L_{MG}}}(\theta) = \frac{2}{\chi(\theta)} \sum_{\text{odd}}^M A_{MG_m} \sin m\theta \quad (15)$$

We stipulate that

$$\frac{C_l}{C_{L_{MG}}}(\theta) \leq \frac{C_{l_{\text{lim}}}}{C_{L_{MG}}}(\theta) \quad (16)$$

The constraint is imposed at  $C_{L_{MG}}$ , which generally will be near stall. Of course, the average  $C_{l_{\text{lim}}}/C_L$  must be greater than unity!

**Parasite Drag**

In the low speed solution, we want to hold the parasite drag equal to that of the elliptical reference wing. Shevell<sup>8</sup> writes the section zero lift drag as

$$C_{d_0} = 2C_f(1 + k_1\tau + k_2\tau^4) \quad (17)$$

One can also add terms involving section  $C_t$ , but their  $t/c$  dependence is negligible; only the  $t/c$ -dependent terms are affected by the optimization. The constraint is that

$$\tau_{\text{ref}} + \frac{k_2}{k_1} \tau_{\text{ref}}^4 = \int_0^{\pi/2} \left( \tau(\theta) + \frac{k_2}{k_1} \tau^4(\theta) \right) \chi(\theta) \sin \theta d\theta \quad (18)$$

$k_2/k_1$  is  $\sim 50$ , but varies with Mach number. In any case, it is a small term; the parasite drag constraint is all but equivalent to fixed frontal area

**Compressibility Drag**

In the high speed solution, we want to fix the drag divergence Mach number  $M_{\text{DIV}}$  is typically 2% larger than the so called crest critical Mach number, a convenient quantity since it can be treated via the following formula, which determines section  $t/c$  as a function of  $C_t$  sweep, and  $M_{\text{cc}}$ :

$$k_r \tau_{\perp} + k_{C_t} C_{t_{\perp}} \sqrt{1 - M_{\text{cc}_{\perp}}^2} = g(M_{\text{cc}_{\perp}}) \quad (19)$$

where

$$\begin{aligned} g(M_{\text{cc}_{\perp}}) &= -1 + \left[ \frac{1 + \sqrt{1 - M_{\text{cc}_{\perp}}^2}}{M_{\text{cc}_{\perp}}} \frac{1}{\sqrt{2 + (\gamma - 1)M_{\text{cc}_{\perp}}^2}} \right. \\ &\quad \left. \times (\sqrt{\gamma + 3 - 2M_{\text{cc}_{\perp}}^2} - \sqrt{(\gamma + 1)(1 - M_{\text{cc}_{\perp}}^2)}) \right] \end{aligned} \quad (20)$$

This expression is derived in Ref 9 based upon thin airfoil and simple sweep aerodynamic approximations with the Karman Tsien pressure correction for compressibility. The constants  $k_r$  and  $k_{C_t}$  characterize airfoils of a family generated by scaling a common thickness envelope and camber line.  $k_r = 1.27$ ,  $k_{C_t} = 0.25$  are typical of good conventional airfoils.

**Minimum  $t/c$** 

The optimization would select vanishing  $t/c$  near the wing tips without the following lower bound:

$$\frac{\tau(\theta)}{\tau_{\text{ref}}} \geq \left( \frac{\tau}{\tau_{\text{ref}}} \right)_{\text{min}} \quad (21)$$

### Aeroelasticity

Aeroelasticity requires somewhat more discussion than the other elements of the wing model. The physical effect to be captured is as follows: When the elastic axis of a swept wing bends, a component of its slope is in the streamwise direction. That introduces effective twist which is approximately proportional to load factor. The twist modifies the bending moments, and so the allowable span. The effect can be included fairly easily if one makes some reasonable approximations: torsion and bending are not coupled; the elastic axis lies on the quarter chord line; and the bending moment at any section is proportional to load factor. (Actually the  $C_{LDD}/C_{LMG}$  ratio has a powerful effect upon the overall optimization precisely because this last statement is not true. However, the nonproportionality is not as important for calculating the incremental load due to elastic deflection.) If one accepts these approximations and applies simple beam theory, then one finds that the elastic twist at 1g is given by

$$\epsilon_E(\theta) = \bar{b}^2 \tan \Lambda \tau_{ref} \epsilon_{TR} \frac{8}{\pi^2} \int_0^{\pi/2} \frac{\sin \theta}{\tau \chi(\theta)} d\theta \quad (22)$$

The scale factor,  $\epsilon_{TR}$ , is the slope along the elastic axis at the tip of the reference wing. One can calculate the incremental lift associated with this twist distribution using the Weissinger aerodynamic method<sup>10</sup> or similar scheme. That combines with the rigid wing additional lift to produce a set of "constant speed"  $A_{Pm}$ :

$$A_{Pm} \triangleq \left(1 - \frac{C_{LE}}{C_{L1g}}\right) A_{Pm} + \frac{C_{LE}}{C_{L1g}} A_{Em} \quad (23)$$

The variation of the  $A_m$  with  $C_L$  at constant speed (i.e., with the load factor proportional to  $C_L$ ) is given by Eq. (3) with  $A_{Pm}$  substituted for  $A_P$ .

Physically, aeroelastic bending shifts lift outboard on a forward swept wing (FSW), and inboard on an aft swept wing (ASW). The tendency, then, is to impose higher bending moments (or lower span) on the FSW, given equal load factors. Somewhat subtler is that elasticity not only changes the spanwise lift distribution, but also increases the FSW's peak total lift in a gust encounter. This effect could be included in the analysis; however, we have treated the fixed load factor case for two reasons: first, it is simpler, involving fewer parameters; second, it corresponds to the practically important case of critical maneuver rather than gust loading.

### Design Formulas and Algorithms

Reference 7 derives the optimal design formulas from our wing model; a review is unnecessary here. Suffice it to say that the following results are formally optimal for the model as presented, at least for rigid wings. Formal optimization with elasticity is analytically intractable, but the solutions in that case still satisfy all constraints and are "good." In fact, on physical grounds it appears that no solution could be significantly better.

This section gives the formulas and evaluation procedure for the two light wing solutions—first the low speed solution with parasite drag constrained, then the high speed solution

with fixed  $M_{cc}$ . The heavy wing solution adds much complication and little illumination; see Ref. 7.

This section gives the formulas and evaluation procedure for the two light wing solutions—first the low speed solution with parasite drag constrained, then the high speed solution with fixed  $M_{cc}$ . The heavy wing solution adds much complication and little illumination; see Ref. 7.

### Light Low Speed Solution

#### Lift

The higher harmonics of the lift series at  $C_{LDD}$  are

$$A_{DDm} = -\frac{4}{\pi^2} \bar{b}^2 \frac{1}{m} \frac{\bar{D}_{DD}}{3(1/\bar{b}^3)} \frac{C_{LDD}}{C_{LMG}} B_m \quad (24)$$

The corresponding span and induced drag are needed to evaluate this formula. The span is determined by the following quadratic:

$$\left(\frac{1}{\bar{b}^3}\right)^2 - \frac{5}{4} \frac{1}{\bar{b}^3} \frac{1}{\bar{b}^3} + \frac{1}{4} \left[\left(\frac{1}{\bar{b}^3}\right)^2 + \left(\frac{2}{\pi} \frac{C_{LDD}}{C_{LMG}}\right)^2 \sum_3^M \frac{B_m^2}{m}\right] = 0 \quad (25)$$

in which

$$\frac{1}{\bar{b}^3} \triangleq \frac{2}{\pi} B_1 + \left(1 - \frac{C_{LDD}}{C_{LMG}}\right) \sum_3^M A_{Pm} B_m \quad (26)$$

The drag at  $C_{LDD}$  satisfies

$$\begin{aligned} \frac{4}{\pi^2} \bar{b}^2 \bar{D}_{DD} &= \left(\frac{C_{LMG}}{C_{LDD}} 3 \frac{1}{\bar{b}^3}\right)^2 \left[1 / \left(2 \sum_3^M \frac{B_m^2}{m}\right)\right] \\ &\times \left\{1 - \left[1 - \left(\frac{4}{\pi} \frac{1}{3(1/\bar{b}^3)} \frac{C_{LDD}}{C_{LMG}}\right)^2 \sum_3^M \frac{B_m^2}{m}\right]^{1/2}\right\} \end{aligned} \quad (27)$$

#### Chord

The chord solution divides the wing into two sections. Over one section (normally inboard), the chord satisfies

$$\begin{aligned} \chi^2(\theta) &= \left[ \frac{2\tau_{ref}}{(8/9) - (\pi/4)} \frac{1}{\tau(\theta)} \sum_{\text{odd}}^M A_{MGm} M_m(\theta) \right] / \left[ \left(1 - \frac{C_{LDD}}{C_{LMG}}\right) \right. \\ &\times \left. \frac{1}{\sin \theta} \sum_3^M B_m \frac{\partial A_{Pm}}{\partial C_m} \sin m\theta - \nu_S \right] \end{aligned} \quad (28)$$

Over the other section, generally outboard, the chord given by this formula is insufficient to satisfy the  $C_t$  bound. The solution then reverts to

$$\chi(\theta) = \frac{2}{C_{lim}(\theta)/C_{LMG}} \sum_{\text{odd}}^M A_{MGm} \sin m\theta \quad (29)$$

The boundary between sections is determined by the Lagrange multiplier  $\nu_S$  in Eq. (28).  $\nu_S$  is set (by iteration) to

**Table 1 Span and drag improvements over an elliptically loaded wing with various weight constraints**

Constraint	Span	Drag	Reference
Root bending moment	1.15	0.85	Jones <sup>1</sup>
Integrated bending moment	1.15	0.89	Prandtl <sup>3</sup>
Integrated bending moment and shear	1.15	0.929	Klein <sup>4</sup>
Integrated $M/t$ wing taper ratio = 0.2	1.042	0.95	Löbert <sup>5</sup>
Integrated $M/t$ , elliptical planform	1.054	0.954	McGeer <sup>7</sup>

satisfy the requirement that the dimensionless chord must integrate to unity.

#### Thickness to Chord Ratio

The  $t/c$  solution also divides the wing into two sections. The formula

$$\tau^2(\theta) = -M(\theta) \left\{ \nu_P \chi^2(\theta) \left( 1 + 4 \frac{k_2}{k_1} \tau^3(\theta) \right) \right\} \quad (30)$$

applies if the resulting  $t/c$  exceeds the lower bound and

$$\tau(\theta) = \tau_{\min}(\theta) \quad (31)$$

otherwise. The Lagrange multiplier is set by the parasite drag constraint

#### Light, High Speed Solution

##### Lift

The low speed solution applies, provided that  $B_m$  in Eq (24) is replaced by  $B'_m$ ,  $m=3,5,\dots,M$  where

$$B'_m \triangleq B_m + \frac{C_{LMG}}{C_{LDD}} \sum_{\text{odd } n} A_{MG_n} T_{nm} \quad (32)$$

and

$$T_{nm} \triangleq \frac{2\tau_{\text{ref}}}{(8/9) - (\pi/4)} 2 \frac{k_{C_t}}{k_r} \frac{C_{LDD}}{\cos\Lambda} \times \int_0^{\pi/2} \frac{M_n(\theta) \sqrt{1 - M_{cc\perp}^2(\theta)}}{(\tau\chi)^2(\theta)} \sin m\theta \sin \theta d\theta \quad (33)$$

##### Chord

Again a Lagrange multiplier divides the wing into two sections. Equation (29) applies where the  $C_t$  constraint is active; otherwise,

$$\begin{aligned} \frac{g(M_{cc\perp}(\theta)) \cos\Lambda}{k_r} \chi(\theta) &= \sqrt{\frac{2\tau_{\text{ref}}}{(8/9) - (\pi/4)} \frac{g(M_{cc\perp}(\theta)) \cos\Lambda}{k_r}} M(\theta) \left/ \left[ \left( 1 - \frac{C_{LDD}}{C_{LMG}} \right) \frac{1}{\sin\theta} \sum_3^M B_m \frac{\partial A_{Pm}}{\partial C_m} \sin m\theta - \nu_s \right] \right. \\ &+ \frac{k_{C_t}}{k_r} \frac{2C_{LDD} \sqrt{1 - M_{cc\perp}^2(\theta)}}{\cos\Lambda} \sum_{\text{odd}} A_{CD_m} \sin m\theta \end{aligned} \quad (34)$$

where

$$B'_m \triangleq B_m + \frac{(C_{LDD} - C_{LDD})}{(C_{LMG} - C_{LDD})} \frac{C_{LMG}}{C_{LDD}} \sum_{\text{odd } n} A_{MG_n} T_{nm} \quad (35)$$

#### Thickness to Chord Ratio

$t/c$  is determined by section lift, chord, and the  $M_{cc}$  constraint, Eq (19):

$$\tau(\theta) = \frac{g(M_{cc\perp}(\theta)) \cos\Lambda}{k_r} - \frac{k_{C_t}}{k_r} \frac{\sqrt{1 - M_{cc\perp}^2(\theta)}}{\cos\Lambda} C_{iCD}(\theta) \quad (36)$$

These sets of low and high speed formulas are the simultaneous equations for the optimal lift, chord and  $t/c$  distributions. Since the formulas are quite nonlinear they must be solved iteratively. An appropriate algorithm is as follows

- 1) Pick an initial planform,  $t/c(\theta)$  and set of  $A_{DDm}$
  - 2) Compute  $A_{Pm}$ ,  $\partial A_{Pm}/\partial C_m$ ,  $C_m$ ,  $A_{MGm}$  and  $C_{LE}$ ,  $A_{Em}$
  - 3) Compute the  $B_m$ ,  $T_{nm}$  and  $B'_m$  Eqs (14) (33) (32)
  - 4) Evaluate the lift distribution formulas Eqs (24) (27)
  - 5) Compute the  $B_m$  [Eq (35)]
  - 6) Evaluate the chord distribution formulas [a) Choose an initial  $\nu_s$  to place the transition between Eq (29), and (28) or (34) about one third semispan from the root b) Calculate the chord c) Integrate the chord d) Adjust  $\nu_s$ , and repeat until the integral is nearly unity]
  - 7) In the high speed case, calculate  $t/c(\theta)$  using Eq (36). In the low speed case use Eqs (30) and (31) and a procedure similar to that for the chord calculation
  - 8) Repeat steps 2-7 until the solution converges
- A set of programs for this and the heavy wing design algorithm, in APL are available upon request

## Optimal Wing Designs

### Light Low Speed Designs

To illustrate the algorithms imagine starting with the unswept elliptical reference wing. Table 2 shows the improvement in span and drag obtained by first optimizing only the lift distribution, then lift and chord, and finally lift, chord and  $t/c$ . The power of the drag design to maximum  $g$   $C_L$  ratio is evident. The spanwise distributions are shown in Figs 1-3. Figure 4 shows the  $C_t$  distribution of one optimized wing.

Little reflection on these figures is needed to appreciate the optimization strategy. Chord and  $t/c$  are distributed grudgingly over the outboard part of the wing in measures just sufficient to satisfy the  $C_t$  and  $t/c$  bounds. That leaves a generous budget for a structurally thick root, which is obviously advantageous. As far as lift is concerned physical reasoning suggests that the lift distribution should be shifted inboard relative to the elliptical standard. All of the optimizations in the literature have confirmed that suggestion, as has this analysis—but only if  $C_{LDD}/C_{LMG}$  is near unity. If however  $C_{LDD}/C_{LMG}$  is significantly less than one the op-

timum shifts back toward elliptical. The reason: in the wing designed for  $C_{LDD} = C_{LMG}$  significant washout twist is needed to produce the inward lift shift at  $C_{LMG}$ . At  $1/3 C_{LMG}$  the effect of that twist is tripled, which makes the tip negatively loaded. Consequently, although the induced drag is relatively low at  $C_{LMG}$ , it is extraordinarily high at  $1/3 C_{LMG}$ . To minimize drag at the lower  $C_L$ , the twist must be reduced which if done optimally returns the lift distribution to a near elliptical form.

One can strike a better balance between lift distributions at low and high  $C_L$ . In fact the lift distributions of the wing with  $C_{LDD}/C_{LMG} = 1$  would be nearly ideal if the  $C_L$ 's were reversed. Two unconventional measures can bring that ideal closer: relaxing the  $C_t$  bound (which allows smaller tip chord and so shifts the additional lift inboard) and sweeping forward. In fact, of all the parameters in the light, low speed optimization only these two have a significant effect. Their effect is large—if the  $C_t$  bound were removed completely then cruise induced drag would be cut by over 20% if  $C_{LDD} = 1/3 C_{LMG}$  (but by only 3% if  $C_{LDD} = C_{LMG}$ ). Unfortunately, in this case mathematics extends far beyond the bounds of physics. Forward sweep is also problematic for low speed wings, since it entails a prohibitive increase in structural over aerodynamic span via the  $\sec\Lambda$  term in Eq

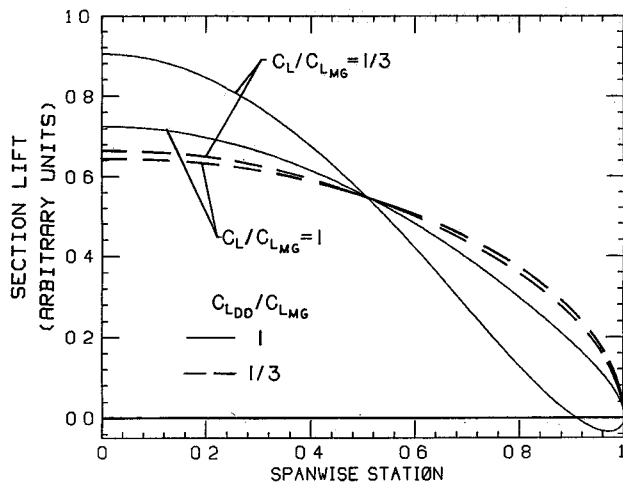


Fig 1 Optimal lift distributions for two low speed wings

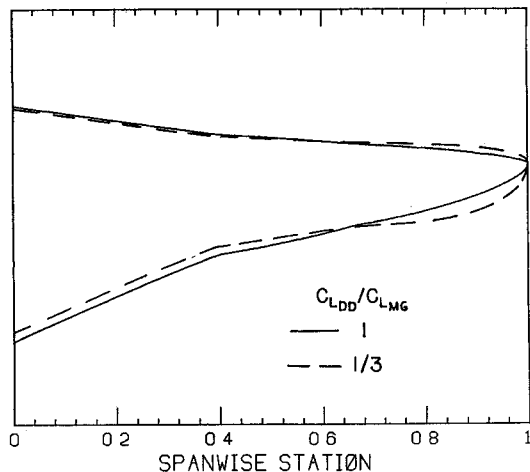


Fig 2 Optimal chord distributions for two low speed wings

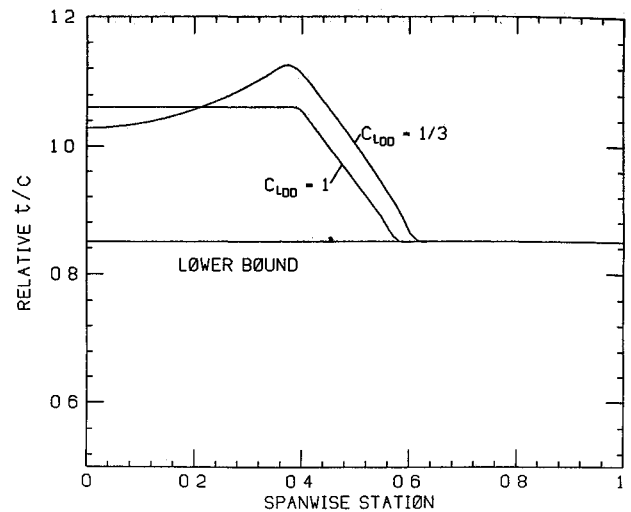
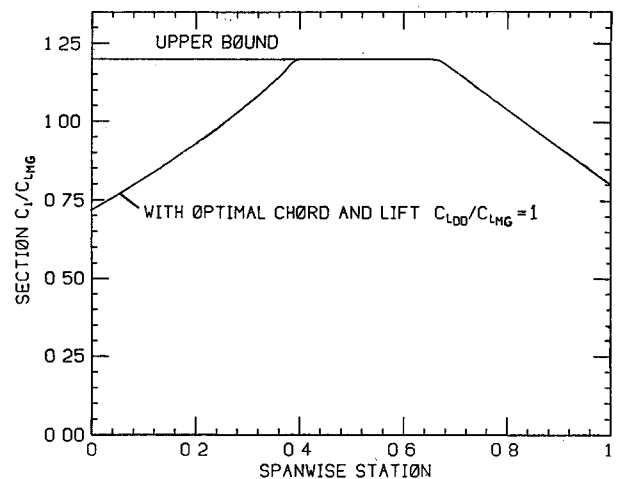
Fig 3 Optimal  $t/c$  distributions for two low speed wings

Fig 4 An optimal distribution of section lift coefficient

(10) But for high speed wings sweep allows an increase in mean  $t/c$ . That effect overcomes the  $\sec\Lambda$  term up to a point, so that maximum span is achieved with some nonzero sweep angle. The result is discussed under light high speed designs.

#### Heavy Low Speed Designs

One can pursue the low speed design problem a bit further by including the wing's own weight in the bending moment. Referring to Fig 5, the parameter  $\bar{W}_S$  is the area weight/total lift. The abscissa is bending weight/total lift. Both are zero in the light wing approximation. As the bending weight increases, the solution bifurcates. Along one branch, the optimal design and its relative performance change little from the optimum light wing (its span increases and its drag decreases due to reduced bending loads but then so do those of an equally heavy elliptical wing). But along the other branch lies a quite remarkable result: the solution favors removing some material from structure and placing it on the tips to relieve the bending moment. Sailplane designers (who have a near monopoly on heavy wings) should take note while being mindful of factors excluded from our analysis (Since sailplanes frequent the high  $C_L$  regime  $C_{L_{DD}}/C_{L_{MG}} = 2/3$  in this example).

#### Light High Speed Designs

Now turn to high speed designs. In light of the discussion above, it is quite fair to say that high speed wings are swept in order to maximize span and so minimize induced drag for a

fixed structural weight. That simple optimization has no preference in the direction of sweep. But three dimensional aerodynamics and aeroelasticity upset the symmetry, as Fig 6 demonstrates. Here we have the span and induced drag (at  $C_{L_{DD}}$ ) of wings optimized for a design condition typical of the Douglas DC 9 30:  $M_{cc} = 0.76$  at  $C_{L_{DD}} = C_{L_{CD}} = 0.4$  with  $C_{L_{MG}} = 1.2$ . Unity on the ordinate represents the best unswept design. Results are shown for three levels of elasticity. The highest level represents DC 9 type construction as determined by fitting our elastic twist formula [Eq (22)] to the actual twist distribution of the DC 9. Of course Eq (22) accounts for scaling with span, sweep, and thickness.

The reason for the difference between forward and aft swept designs becomes apparent upon comparison of the lift distributions of optimized 30 deg forward and aft swept designs at  $C_{L_{DD}}$  and  $C_{L_{MG}}$ . These are plotted in Fig 7. At  $C_{L_{DD}}$  their lift distributions are almost identical but at  $C_{L_{MG}}$  the lift is shifted inboard on the FSW, and outboard on the ASW. These opposite lift shifts reflect opposite additional lift characteristics. One can see physically that this difference in itself would give the FSW an advantage. But furthermore it has a synergistic effect when combined with the  $C_l$  bound and  $M_{cc}$  constraint (Incidentally, in these calculations the stipulated  $M_{cc}$  increased by about 10% from root to tip). Figures 8 and 9 indicate the result: a thicker inboard section in the FSW which allows still larger span. Now the FSW has the handicap of positive aeroelastic feedback in the bending

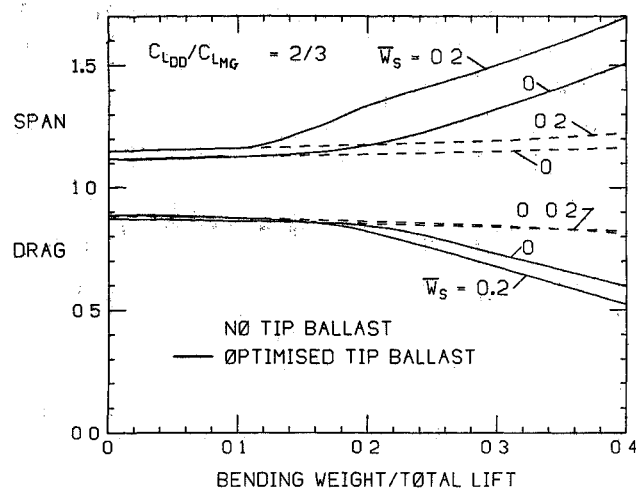


Fig 5 Induced drag (at  $C_{LDD}$ ) and span of optimized heavy wings relative to equally heavy elliptical wings

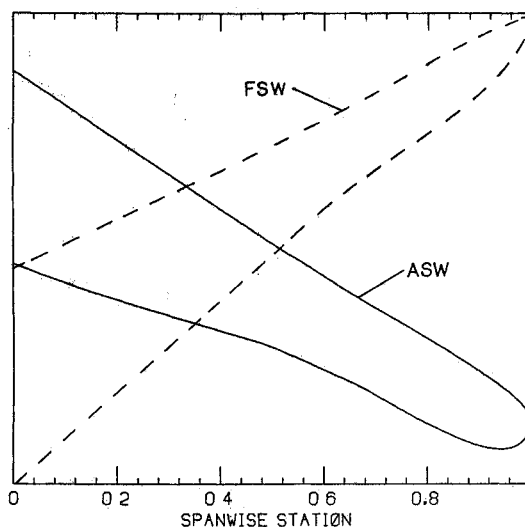


Fig 8 Optimal chord distributions for high speed wings with 30 deg forward and aft sweep.

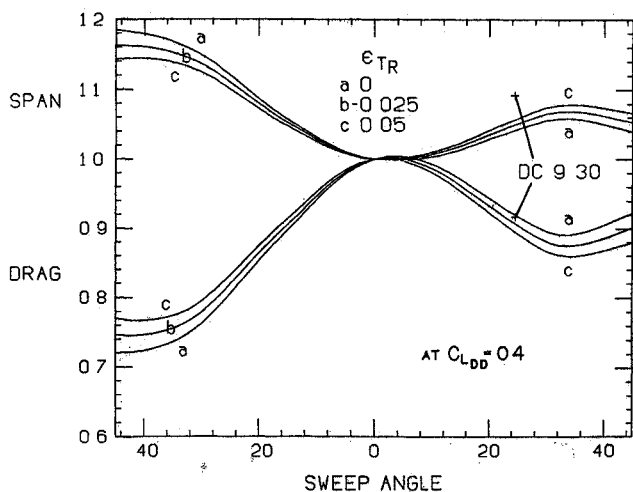


Fig 6 Induced drag (at  $C_{LDD}$ ) and span of high speed wings as a function of sweep and elasticity;  $M_{cc}=0.76$  at  $C_{LCD}=0.4$  with  $C_{LDD}/C_{LMG}=1/3$

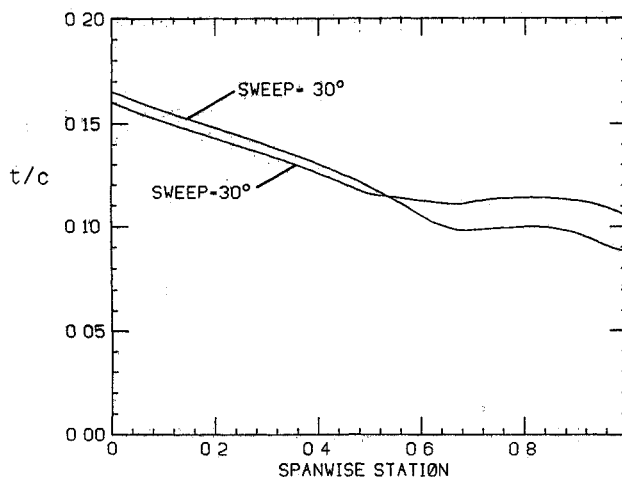


Fig 9 Optimal  $t/c$  distributions for high speed wings with 30 deg forward and aft sweep

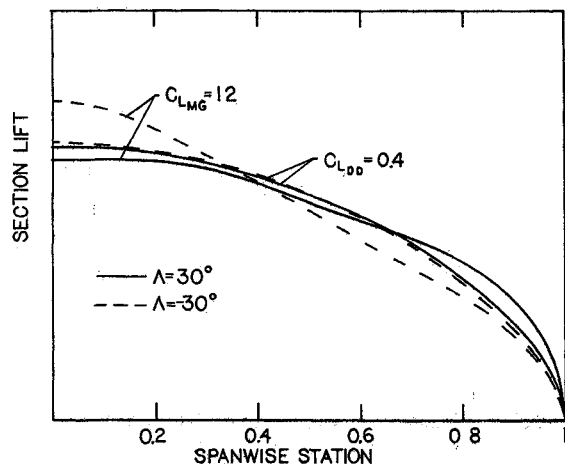


Fig 7 Optimal lift distributions for high speed wings with 30 deg forward and aft sweep

moment; that reduces its advantage over the ASW from 16% with a rigid wing to 9% with  $\epsilon_{TR}=0.05$  and 30 deg sweep. These figures apply at  $C_{LDD}$ ; because of the FSW's substantial inboard lift shift and consequent reduction in span efficiency with increasing  $C_L$ , the drag advantage decreases to about 3% at  $C_{LMG}$ .

This analysis offers a new perspective on the choice of sweep angle for high speed wings, which should be weighed with the many other factors which normally influence the decision. It is appropriate to mention a few of these. For further discussion, see, for example, Refs 11-13. Advantages of forward sweep include superior stall characteristics due to inward rather than outward motion of the upper surface boundary layer; possibly lower parasite drag for a given quarter-chord sweep, due to lower leading-edge sweep; and possibly higher  $M_{cc}$  for a given quarter chord sweep, due to higher sweep of the shock surface. Disadvantages of forward sweep include: pitch up tendency with root-first stall; possible interference drag due to coalescence of the wing and fuselage boundary layers; and problematic undercarriage stowage (Longitudinal dynamic analysis<sup>7</sup> indicates that the aerodynamic centers of forward and aft swept wings should be placed in almost the same position relative to the fuselage/tail center of gravity. That might leave the FSW's root uncomfortably far aft for main gear placement.)

**Table 2 Span and drag improvements over an elliptically loaded wing given by the light, low speed optimization**

$C_{LDD}$ $C_{LMG}$	Optimized lift only		Optimized lift and planform		Optimized lift planform and $t/c$	
1	1 054 span	0 954 drag	1 121 span	0 863 drag	1 136 span	0 850 drag
1/3	1 004 span	0 996 drag	1 050 span	0 910 drag	1 062 span	0 891 drag

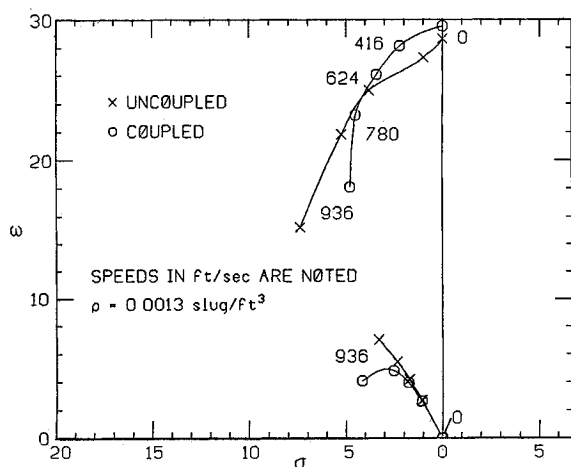


**Fig 10 Root locus vs speed of pitch/plunge/bending eigenvalues for a typical transport with the optimized 30 deg forward swept wing**

### Flutter

Forward-swept wings are prone to a flutter mode which deserves special attention. In some cases an oscillatory instability can occur at a speed lower than that for divergence in bending. The instability involves coupling between the primary wing bending mode and rigid body pitch/plunge (short period mode). The frequency of the latter generally increases with increasing speed, while the former decreases. At some point the frequencies become close enough to couple and an unstable oscillation develops.

Weisshaar and Zeiler<sup>14</sup> have calculated this behavior for a system with parameters reminiscent of Grumman's X-29 fighter demonstrator. We have done an analysis using a different approach (involving simultaneous solution for the elastic mode shapes and eigenvalues) which gives similar results with similar parameters. However, with parameters characteristic of a DC-9 type aircraft, a qualitatively different result is obtained. Figure 10 shows the root locus of bending and short period eigenvalues vs speed at a relatively low altitude (the critical case). "Uncoupled" implies clamped root wing bending and rigid wing short period modes. The speeds noted correspond to Mach numbers of 0.4, 0.6, 0.75, and 0.9. No instability occurs in this speed range; however, instability can be demonstrated by increasing the flexibility parameter ( $\epsilon_{TR}$ ) in the analysis. That shows divergence occurring before oscillatory instability. The difference between Weisshaar's example and those herein apparently arises because of the higher pitch damping inherent in a transport type configuration. Evidently the pitch/plunge/bending flutter is not a problem in such configurations.

### Conclusions

The algorithms presented herein allow systematic selection of spanwise lift chord,  $t/c$  and material distributions. The selection is optimal in our idealized design problems—and we presume "good" in real design problems—in that it minimizes induced drag subject to constraints on structural weight, local  $C_l$ , and parasite or compressibility drag. The objective in developing these algorithms has been to find

improvements in current design practice. Exploration has revealed some promising strategies.

For low speed wings, a drag reduction on the order of 15% can be realized relative to a wing with elliptical span loading and planform and constant  $t/c$ . However, the fairly modest design revisions favored by our analysis (mostly in planform and  $t/c$ ) have been appreciated for many years, therefore, improvements over current practice are generally less impressive. Heavy wings in which the wing weight is a significant fraction (say more than 20%) of the total lift are exceptional. With these wings (found almost exclusively in sailplanes) an induced drag reduction as large as 20% might be achieved by removing some structural material to the tips. It is more valuable relieving than carrying the bending moment.

For high speed wings, best results are achieved when our algorithms are combined with optimal choice of sweep. The principal conclusion of our high speed optimization is that in many practical applications, even with elasticity characteristic of conventional design practice, an optimized forward swept wing can offer significantly lower induced drag in cruise (say 10%) than an aft swept wing designed for the same load factor.

### References

- Jones, R. T., "The Spanwise Distribution of Lift for Minimum Induced Drag of Wings Having a Given Lift and Root Bending Moment," NACA TN 2249, Dec 1950.
- de Young, J., "Minimization Theory of Induced Drag Subject to Constraint Condition," NASA CR 3140, June 1979.
- Prandtl, L., "Über tragflügel des kleinsten induzierten widerstandes," *Zeitschrift für Flugtechnik und motorluftschiffahrt*, 24 Jg 1933 (Reprinted edited by W. Tollmein, H. Schlichting, and W. Gortler, *Gesammelte Abhandlungen*, Springer Verlag, Berlin 1961).
- Klein, A. and Viswanathan, S. P., "Approximate Solution for Minimum Induced Drag of Wings with Given Structural Weight," *Journal of Aircraft*, Vol 12, Feb 1975, pp 124-126.
- Löbert, G., "Spanwise Lift Distribution of Forward and Aft Swept Wings in Comparison with the Optimum Distribution Form," *Journal of Aircraft*, Vol 18, June 1981, pp 496-498.
- McGeer, T. and Kroo, I., "A Fundamental Comparison of Canard and Conventional Configurations," *Journal of Aircraft*, Vol 20, Nov 1983, pp 983-992.
- McGeer, T., "Wing Design for Minimum Drag with Practical Constraints," Ph.D. Dissertation, Stanford University, Stanford, Calif., Dec 1983.
- Shevell, R., "Notes for Aerospace Systems Synthesis and Analysis," Department of Aeronautics and Astronautics, Stanford University, Stanford, Calif., 1979.
- McGeer, T. and Shevell, R., "A Method for Estimating the Compressibility Drag of an Airplane," Stanford University, Stanford, Calif., SUDAAR 535, Jan 1983.
- de Young, J. and Harper, C. W., "Theoretical Symmetric Span Loading at Subsonic Speeds for Wings having Arbitrary Plan Form," NACA Rept 921, 1948.
- Uhuad, G. C., Weeks, T. M., and Large, R., "Wind Tunnel Investigation of the Transonic Aerodynamic Characteristics of Forward Swept Wings," *Journal of Aircraft*, Vol 20, March 1983, pp 195-202.
- Hoerner, S. F., "Fluid Dynamic Lift," Hoerner Fluid Dynamics, Brick Town, 1975, Chaps 15 and 16.
- Grafton, S. B. et al., "High Angle of Attack Characteristics of a Forward Swept Wing Fighter Configuration," *Proceedings of the AIAA 9th Atmospheric Flight Mechanics Conference*, Aug 1982.
- Weisshaar, T. A. and Zeiler, T. A., "Dynamic Stability of Flexible Forward Swept Wing Aircraft," *Proceedings of the AIAA 9th Atmospheric Flight Mechanics Conference*, Aug 1982.